Electronic Supplementary Information

Electrically tuned hyperfine spectrum in neutral Tb(II)(Cp^{iPr5})$_2$ single-molecule magnet

Robert L. Smith,[1] Aleksander L. Wysocki,[2,*] and Kyungwha Park[2,†]

[1] *Department of Chemistry, Virginia Tech, Blacksburg, Virginia 24061, United States*
[2] *Department of Physics, Virginia Tech, Blacksburg, Virginia 24061, United States*

(Dated: September 10, 2020)

* alexwysocki2@gmail.com
† kyungwha@vt.edu

CONTENTS

I. ACTIVE SPACE STUDY

TABLE S1: State-average occupation numbers of the optimized active orbitals in different CASSCF calculations in the high-spin state of the neutral Tb(II)(Cp^{iPr5})$_2$ molecule. State-averaging is done over the lowest 21 roots except for CASSCF(9,8) where only the seven lowest roots are used. The seven Tb $4f$ active orbitals are not listed since in all cases the state-average occupation number of each $4f$ orbital is 1.143. Note that the CASSCF(9,13) and CASSCF(9,15) results use frozen orbitals from the CASSCF(9,12) calculation.

CASSCF	State-average occupation numbers
CASSCF(9,8)	($5d_{z^2}, 5d_{x^2-y^2}, 5d_{xy}, 6s$) (1.000)
CASSCF(9,10)	($5d_{z^2}, 6s$) (0.333), $5d_{x^2-y^2}$ (0.333), $5d_{xy}$ (0.333)
CASSCF(9,12)	($5d_{z^2}, 6s$) (0.333), $5d_{x^2-y^2}$ (0.333), $5d_{xy}$ (0.333), $5d_{xz}$ (0.001), $5d_{yz}$ (0.001)
CASSCF(9,13)	($5d_{z^2}, 6s$) (0.333), $5d_{x^2-y^2}$ (0.333), $5d_{xy}$ (0.333), $5d_{xz}$ (0.001), $5d_{yz}$ (0.001), $6s$ (0.000)
CASSCF(9,15)	($5d_{z^2}, 6s$) (0.333), $5d_{x^2-y^2}$ (0.333), $5d_{xy}$ (0.333), $5d_{xz}$ (0.001), $5d_{yz}$ (0.001), $6p_x$ (0.000), $6p_y$ (0.000), $6p_z$ (0.000)
CASSCF(13,14)	L1 (1.993), L2 (1.993), ($5d_{z^2}, 6s$) (0.333), $5d_{x^2-y^2}$ (0.333), $5d_{xy}$ (0.333), $5d_{xz}$ (0.008), $5d_{yz}$ (0.008)

In order to determine the optimal active space for the neutral Tb(II)(Cp^{iPr5})$_2$ molecule, we focus on the high spin state and perform a series of test CASSCF calculations with different types of active orbitals. In the first step we analyze which Tb-based orbitals should be included in the active space. We start with a CASSCF(9,12) calculation with 9 active electrons and 12 active orbitals that consists of 7 Tb $4f$ and 5 Tb $5d$ orbitals. The optimized orbitals obtained using state-average procedure over the lowest 21 roots (see the main text) consist of 7 atomic-like $4f$ orbitals, a ($5d_{z^2}, 6s$) hybrid orbital as well as $5d_{xy}$, $5d_{xz}$, $5d_{yz}$, and $5d_{x^2-y^2}$ orbitals. The optimized ($5d, 6s$) orbitals are very similar to the ones shown in Fig. 2 of the main text. In particular, the $5d_{xy}$, $5d_{xz}$, $5d_{yz}$, and $5d_{x^2-y^2}$ orbitals show significant hybridization with $2p_z$ orbitals from the Cp rings. The obtained state-average occupation numbers of the optimized active orbitals are listed in Table S1 and the corresponding spin-free energies are shown in Table S2. The state-average occupation numbers of all $4f$ orbitals are ~ 1.143. This corresponds to the expected configuration of eight electrons residing on the $4f$ shell. On the other hand, the $5d$ and $6s$ orbitals have non-equal state-average occupation numbers. Each of the ($5d_{z^2}, 6s$), $5d_{x^2-y^2}$, and $5d_{xy}$ orbitals has a state-average occupation number of 0.333, while each of the $5d_{xz}$ and $5d_{yz}$ orbitals has almost zero occupation number. For the spin-free CASSCF(9,12) ground state, ($5d_{z^2}, 6s$) is almost singly occupied, whereas the rest of the $5d$ orbitals have almost zero occupation. However, it is not enough to include only the ($5d_{z^2}, 6s$) orbital in the active space. Indeed, our CASSCF(9,8) calculation (using state-average over the 7 lowest roots) with merely 7 $4f$ orbitals and the ($5d_{z^2}, 6s$) orbital in the active space, shows that spin-free CASSF(9,8) energies dramatically differ from the spin-free CASSCF(9,12) energies (Table S2). In addition, the initial ($5d_{z^2}, 6s$) active orbital in the CASSCF(9,8) calculation acquires significant contributions of $5d_{x^2-y^2}$ and $5d_{xy}$ orbitals upon orbital optimization. The fact that $5d_{xz}$ and $5d_{yz}$ orbitals have small occupation numbers in the above CASSCF(9,12) calculation suggests that these orbitals could be potentially removed from the active space. Therefore, we perform a CASSCF(9,10) calculation where only ($5d_{z^2}, 6s$), $5d_{x^2-y^2}$, and $5d_{xy}$ orbitals are included in the active space in addition to 7 $4f$ orbitals. The resulting spin-free energies, however, differ significantly

from the CASSCF(9,10) energies (Table S2). This indicates that the $5d_{xz}$ and $5d_{yz}$ orbitals should be retained in the active space despite their low occupation numbers.

Next, we perform a CASSCF(9,13) calculation. Here the active space is like in the CASSCF(9,12) calculation but with additional Tb $6s$-like orbital. In turns out, however, that during the self-consistent orbital optimization the $6s$-like orbital is removed from the active space and is replaced by Tb $5f$, Tb $5g$, or even ligand orbitals. Therefore, a CASSCF(9,13) calculation is performed with frozen orbitals from the CASSCF(9,12) calculation (using the Molcas keyword `CIONLY`). Here, the $6s$ orbital is strongly hybridized with the ligand orbitals. As shown in Table S1, the occupation number of the $6s$ orbital is virtually zero. This suggests that this orbital does not need to be included in the active space. Indeed, the spin-free energies of the CASSCF(9,13) calculation differ from the CASSCF(9,12) energies by less than 1 cm^{-1} (Table S2). A similar procedure is followed to find out whether the Tb $6p$ orbitals should be included in the active space. We perform a CASSCF(9,15) calculation with the active space like in the CASSCF(9,12) calculation but with additional $6p_x$, $6p_y$, and $6p_z$ orbitals. Since the $6p$ orbitals are removed from the active space during the self-consistent orbital optimization, we use frozen orbitals from the CASSCF(9,12) calculation. The initial $6p$ active orbitals are strongly hybridized with the ligand orbitals. The inclusion of the $6p$ orbitals in the active space modifies the spin-free energies by several tens cm^{-1} (Table S2). Nevertheless, the occupation numbers of the $6p$ orbitals are zero (Table S1). Therefore, we do not include the Tb $6p$ orbitals in the active space.

TABLE S2: Relative spin-free energies for different CASSCF calculations in the high-spin state of the neutral Tb(II)$(Cp^{iPr5})_2$ molecule. State-averaging is done over the lowest 21 roots except for CASSCF(9,8) where only the 7 lowest roots are used. All energies are in units of cm^{-1}. Note that the CASSCF(9,13) and CASSCF(9,15) calculations use frozen orbitals from the CASSCF(9,12) calculation.

State	CAS(9,8)	CAS(9,10)	CAS(9,12)	CAS(9,13)	CAS(9,15)	CAS(13,14)
1	0.0	0.0	0.0	0.0	0.0	0.0
2	51.5	0.1	3.6	3.6	3.9	0.1
3	79.0	755.4	653.8	653.6	690.2	765.3
4	186.4	804.7	699.2	699.1	734.8	814.5
5	960.9	1509.4	1336.2	1336.3	1399.0	1499.2
6	1479.8	1770.7	1570.3	1570.3	1619.7	1777.7
7	1903.2	1791.4	1641.5	1641.5	1695.5	1796.8
8		2044.3	1984.2	1984.1	2032.2	2061.3
9		2432.0	2205.8	2205.8	2267.2	2205.3
10		2434.4	2210.8	2210.9	2272.0	2213.3
11		2536.8	2252.6	2552.7	2598.2	2463.2
12		2540.9	2563.5	2563.5	2608.6	2466.0
13		2956.2	2825.0	2824.9	2843.2	2853.1
14		2957.6	2829.3	2829.2	2847.7	2855.0
15		3245.8	3185.5	3185.4	3189.7	3162.7
16		3285.4	3226.8	3226.7	3231.3	3207.9
17		3342.2	3479.0	3479.2	3546.0	3394.7
18		3343.0	3479.6	3479.7	3546.6	3395.4
19		5591.2	5457.5	5457.1	5438.8	5382.4
20		5609.6	5472.8	5472.4	5448.2	5402.8
21		5668.0	5643.0	5642.3	5631.5	5518.7

Having established which Tb-based orbitals should be included in the active space, we now focus on the ligand-type orbitals. In principle, all π/π^* orbitals from the Cp rings are potential candidates to include in the active space. This is, however, computationally prohibitive. Therefore, in order to determine whether and which ligand orbitals should be included in the active space, we use the energies of the CASSCF(9,12) ligand orbitals and the strength of hybridization with Tb-based orbitals. In particular, among the occupied ligand orbitals, there are four highest lying π-like orbitals that are separated by a gap larger than 0.1 Ha from the lower-lying orbitals. Among these four orbitals, two orbitals (denoted as L1 and L2) hybridize with the Tb $5d_{xz}$ and $5d_{yz}$ orbitals, while the other two orbitals (denoted as L3 and L4) hybridize with the Tb $6p_x$ and $6p_y$ orbitals. In order to test an importance of the presence of the L1 and L2 orbitals in the active space, we perform a CASSCF(13,12) calculation with the active space including L1 and L2 orbitals as well as seven $4f$ orbitals and $(5d_{z^2}, 6s)$, $5d_{x^2-y^2}$, and $5d_{xy}$ orbitals. Note that since the L1 and L2 orbitals are nominally doubly occupied, the active space consists of 13 electrons. During the CASSCF(13,12) orbital optimization, however, the L1 and L2 orbitals are removed from the active space and they are replaced by the Tb $5p_{x,y}$ orbitals. In order to stabilize the presence of L1 and L2 orbitals in the active space, $5d_{xz}$ and $5d_{yz}$ orbitals need to be included in the active space as well. Indeed, a CASSCF(13,14) calculation with additional $5d_{xz}$ and $5d_{yz}$ orbitals in the active space converges successfully with L1 and L2 orbitals staying in the active space. The result of

such CASSCF(13,14) calculation is shown in Tables S1 and S2. As seen, while the occupation numbers of the L1 and L2 orbitals only slightly differ from two, the inclusion of the L1 and L2 orbitals in the active space has a significant effect on the spin-free energies. Next, we consider the L3 and L4 orbitals. Again, a CASSCF(13,12) calculation with L3 and L4 orbitals in the active space in addition to $(5d_{z^2}, 6s)$, $5d_{x^2-y^2}$, $5d_{xy}$, and 7 $4f$ orbitals, does not converge and during self-consistent orbital optimization procedure the L3 and L4 orbitals are replaced by the Tb $5p_{x,y}$ orbitals. In order to stabilize the L3 and L4 orbitals in the active space, we perform a CASSCF(13,13) calculation with 7 $4f$, 3 $6p$, $(5d_{z^2}, 6s)$, L3, and L4 orbitals in the active space. The L3 and L4 orbitals, however, are also removed from the active space as well as the $6p$ orbitals. This is consistent with our previous finding that the Tb $6p$ orbitals do not need to be included in the active space. Regarding the empty π^*-like orbitals, they lie high in energy far away from the active orbitals and, thus, we do not include them in the active space. Therefore, we conclude that the CAS(13,14) consisting of 7 Tb $4f$, Tb $5d_{xy}$, $5d_{xz}$, $5d_{yz}$, $5d_{x^2-y^2}$, $(5d_{z^2}, 6s)$, and two nominally doubly-occupied ligand orbitals (L1 and L2) is the optimal active space for the neutral Tb(II)$(Cp^{iPr5})_2$ molecule.

II. SPIN-FREE ENERGIES OF HIGH- AND LOW-SPIN STATES

TABLE S3: Relative energies of the high-spin (HS) and low-spin (LS) spin-free (SF) states obtained from CASSCF(13,14) calculations. Here, the HS (LS) state has spin $S = 7/2$ ($S = 5/2$). The energy of the first HS SF state is lower than that of the first LS SF state by 6069.8 cm^{-1}.

SF state	HS Relative Energy (cm^{-1})	LS Relative Energy (cm^{-1})
1	0.0	0.0
2	0.1	0.3
3	765.3	852.1
4	814.5	1117.6
5	1499.2	1123.9
6	1777.7	1435.0
7	1796.8	1466.5
8	2061.3	2136.9
9	2205.3	2137.6
10	2213.3	3002.3
11	2463.2	3002.9
12	2466.0	3554.6
13	2853.1	3671.8
14	2855.0	3816.7
15	3162.7	3820.4
16	3207.9	4052.8
17	3394.7	4181.8
18	3395.4	4210.9
19	5382.4	4732.2
20	5402.8	4892.1
21	5518.7	4895.8

III. CASSCF(13,14)-RASSI-SO ENERGIES

TABLE S4: Relative energies of the several tens lowest CASSCF(13,14)-SO-RASSI states. Here, only 21 lowest CASSCF(13,14) roots for the high-spin state are included in the RASSI-SO calculations.

SO-RASSI state	HS Relative Energy (cm^{-1})
1	0.0
2	0.0
3	311.0
4	311.0
5	583.5
6	583.5
7	795.9
8	795.9
9	939.4
10	939.4
11	1044.7
12	1044.7
13	1104.3
14	1104.3
15	1154.6
16	1154.6
17	1212.2
18	1212.2
19	1272.0
20	1272.0
21	1340.7
22	1340.7
23	1740.6
24	1740.6
25	2595.8
26	2595.8
27	2615.2
28	2615.2
27	2647.9
28	2647.9
29	2669.1
30	2669.1
31	2678.9
32	2678.9
33	2733.8
34	2733.8

IV. MAGNETIC PROPERTIES

Using the calculated CASSCF(13,14)-SO-RASSI energies and wave functions within the SINGLE_ANISO program, we calculate powder magnetization (M) versus H field at different temperatures (2-30 K) (Fig. S1) and the product of the powder magnetic susceptibility with the temperature ($\chi_M T$) as a function of temperature T at $H = 0.1$ T (Fig. S2). No fitting parameters are used in the calculations ($zJ' = 0$ in SINGLE_ANISO). The magnetization data agree well with the experimental data on a diluted sample (Fig. S75 in Ref. 1). On the other hand, for $\chi_M T$, there are differences between the calculations (Fig. S2) and the experiment (Fig. S15 in Ref. 1). In particular, the calculated $\chi_M T$ at 300 K is 14.15 emu K/mol compared to the experimental value of 12.72 emu K/mol.[1] Note that the susceptibility measurements were not reported for diluted samples[1] and that it can be affected by intermolecular interaction. The intermolecular interactions can be at least partially responsible for the discrepancy between the experimental data and our calculations performed for an isolated molecule. This seems to be the case especially at low temperatures where a good agreement between theory and experiment on a diluted sample is achieved for the powder magnetization data. The lack of dynamic correlation in the calculations can also contribute to the differences between theory and experiment. The dynamic correlation can reduce the energy difference between the high-spin and low-spin ground states, which can affect the susceptibility. In order to illustrate this effect we perform CASSCF(13,14)-RASSI-SO calculations with an extra overall upward energy shift (V_S) applied to the high-spin CASSCF(13,14) states.

This shifts lowers the energy difference between the high-spin and low-spin CASSCF(13,14) states. Fig. S3 shows $\chi_M T$ for two different values of the upward shift (in units of Hartree) and compares with the calculations without the shift. As shown, the shift leads to a reduction of the room-temperature $\chi_M T$ value that becomes closer to the experiment. A larger shift is equivalent to a smaller energy difference between the high-spin and low-spin ground states. We note, however, that the adapted shifts are arbitrary and the purpose of Fig. S3 calculations is only to illustrate an importance of the effect of the energy level renormalization due to to dynamic correlation.

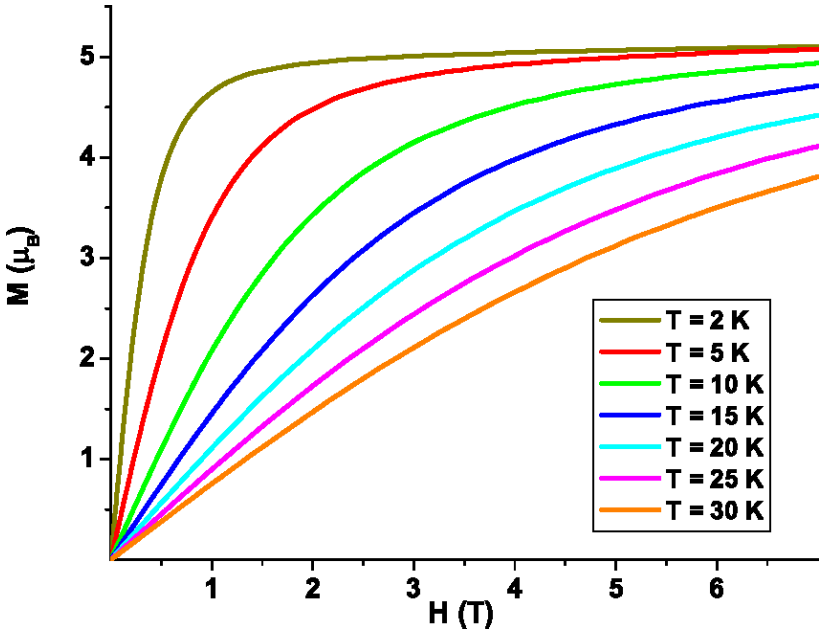

FIG. S1: **H**-field dependence of the magnetization at different temperatures calculated using the SINGLE_ANISO module in the Molcas code based on the CASSCF(13,14)-RASSI-SO calculations. Our calculated result agrees with the experimental data (Fig.S75 in Ref.[1]) with toulene which separates individual Tb(II)$(Cp^{iPr5})_2$ molecules.

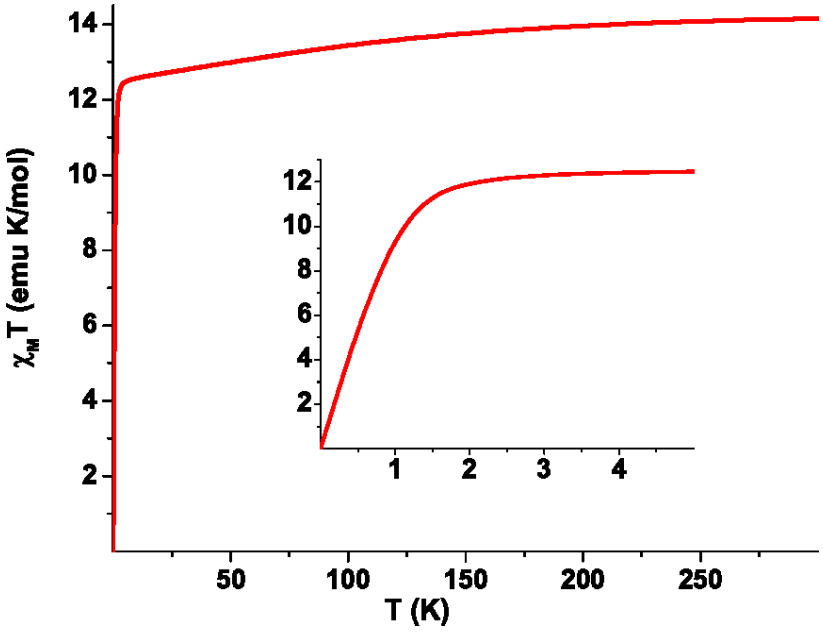

FIG. S2: Temperature (T) dependence of the magnetic susceptibility calculated using the SINGLE_ANISO module of the Molcas code based on the CASSCF(13,14)-RASSI-SO calculations. The susceptibility is evaluated as a ratio of the magnetization to the **H** field at **H** =0.1 T. The inset shows the low-temperature region of the plot. The result differs somewhat from the available experimental data (Fig.S15 in Ref.[1]) due intermolecular interactions present in the experiment and absence of dynamic correlation in the calculations.

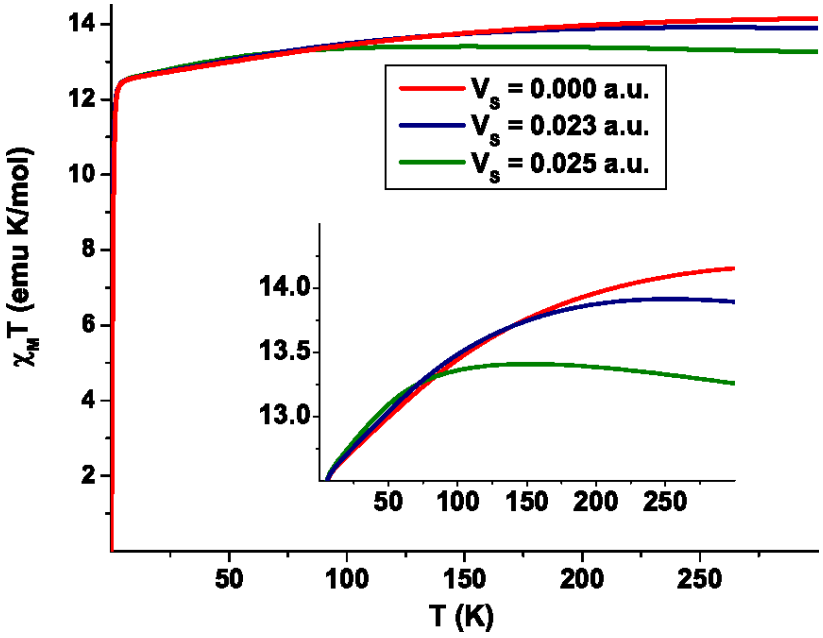

FIG. S3: Temperature dependence of the magnetic susceptibility calculated using the SINGLE_ANISO module of the Molcas code based on the CASSCF(13,14)-RASSI-SO calculations. The susceptibility is evaluated as a ratio of the magnetization to the **H** field at **H** =0.1 T. Different curves correspond to different upward energy shifts (in units of Hartree) applied to the high-spin CASSCF(13,14) states in the RASSI-SO calculations. The inset shows the high-susceptibility region of the plot. While the shifts improve agreement with the experimental room temperature value of $\chi_M T$, they introduce a slightly non-monotonic temperature dependence of $\chi_M T$.

[1] C. A. Gould, K. R. McClain, J. M. Yu, T. J. Groshens, F. Furche, B. G. Harvey, and J. R. Long, J. Am. Chem. Soc. **141**, 12967 (2019).